

# Quantized symbolic time series approximation

Erin Carson<sup>1</sup>, Xinye Chen<sup>2\*</sup>, Cheng Kang<sup>3†</sup>

<sup>1</sup>Department of Numerical Mathematics, Charles University, Prague, Czech Republic.

<sup>2\*</sup>LIP6, Sorbonne Université, CNRS, Paris, France.

<sup>3</sup>Department of Cybernetics, Czech Technical University in Prague, Prague, Czech Republic.

\*Corresponding author(s). E-mail(s): [xinye.chen@lip6.fr](mailto:xinye.chen@lip6.fr);

Contributing authors: [carson@karlin.mff.cuni.cz](mailto:carson@karlin.mff.cuni.cz); [kangchen@fel.cvut.cz](mailto:kangchen@fel.cvut.cz);

<sup>†</sup>These authors contributed equally to this work.

## Abstract

Time series are ubiquitous in numerous science and engineering domains, e.g., signal processing, bioinformatics, and astronomy. Previous work has verified the efficacy of symbolic time series representation in a variety of engineering applications due to its storage efficiency and numerosity reduction. The most recent symbolic aggregate approximation technique, ABBA, has been shown to preserve essential shape information of time series and improve downstream applications, e.g., neural network inference regarding prediction and anomaly detection in time series. Motivated by the emergence of high-performance hardware which enables efficient computation for low bit-width representations, we present a new quantization-based ABBA symbolic approximation technique, QABBA, which exhibits improved storage efficiency while retaining the original speed and accuracy of symbolic reconstruction. We prove an upper bound for the error arising from quantization and discuss how the number of bits should be chosen to balance this with other errors. We present an application of QABBA combined with large language models (LLMs) for time series regression, exploring its effectiveness. By encoding time series as symbolic pattern chains, QABBA eliminates the need to train embeddings from scratch and achieves state-of-the-art results on the Monash regression dataset. This symbolic approximation enhances the efficiency of fine-tuning LLMs for time series regression across diverse domains. Extensive experiments on well-established datasets further highlight the benefits of QABBA’s symbolic approach.

**Keywords:** symbolic approximation, time series representation, quantization, time series regression, language models

# 1 Introduction

The ubiquity of temporally annotated data produced, e.g., by Internet of Things devices, demands efficient storage and transfer of time series data. Time series are of naturally high numerosity and often have complex characteristics. The curse of dimensionality [1] limits almost all data mining and machine learning algorithms when dealing with large-scale data since they scale poorly with dimensionality. Therefore, to store and analyze vast amounts of data, efficient management and mining of time series are critical in modern science and engineering domains; see [2] for survey. Numerous data mining and compression techniques have been developed to aid time series analysis in an elegant manner; see [3] and [4] for references. Computing a representation that reduces the numerosity while preserving the essential characteristics of time series often leads to an enhancement in algorithm performance and dramatically mitigates the pressure on compute resources. Well-established representations include, but are not limited to, i.e., functional approximation (based on the discrete Fourier transform [5], discrete wavelet transform [6], subband coding [7], or piecewise linear representations [8]) and *symbolic approximation* (based on SAX [9], 1d-SAX [10], ABBA [11] or FABBA [12]).

As mentioned in [13], numerical-based representations are real-valued, which limits the potential algorithms and data structures. An alternative is to utilize the symbolic representation (generated by symbolic approximation), the efficacy of which has been substantiated by various downstream applications, e.g., anomaly detection [11, 14], classification [15], forecasting [16, 17], motif discovery [18], event prediction [19], and clustering [20]. In this paper, we focus on the adaptive Brownian bridge-based symbolic aggregation (ABBA), a symbolic approximation technique that was recently introduced in [11]. ABBA performs time series discretization with numerosity reduction (often referred to as dimensionality reduction), which enables efficient algorithmic manipulation in a low-dimensional space, and the representation enables the semantic information of time series to be utilized.

Our method is motivated by techniques used for model *quantization* in deep neural network training. Quantization is a well-established method for reducing the bit-width of the number format—by converting floating point numbers into integers—such that storage and computational costs can be reduced. Often, integer-based arithmetic, such as integer matrix multiplication, can run much faster than conventional floating point arithmetic in commonly available hardware supporting integer arithmetic (e.g., x86 CPUs and ARM NEON), and particularly in specialized hardware implementations (e.g., UNPU [21], Eyeriss [22], Pragmatic [23]) and specialized hardware instructions (e.g., NVIDIA Tensor cores). Related surveys on neural network quantization can be found in [24, 25]. Due to the appealing simplicity, this method can be seamlessly integrated into the ABBA methods without compromising the applications compared to other existing compression method.

In this paper we aim to design a method that can approximate time series in a meaningful, storage-efficient representation that can be applied to various downstream applications. To do so, we apply the ideas of quantization to ABBA-based methods for the symbolic approximation of time series data. The primary contributions of the present work are:

1. We introduce a quantization technique seamlessly into the ABBA method, which effectively improves the storage efficiency while significantly retaining the accuracy and speed of the symbolic approximation. The essential idea of our proposed method is to use low bit-width integer types to replace the symbolic centers stored in working precision (often single or double precision), which enables a more storage-efficient symbolic representation compared to ABBA. We call our method QABBA, for quantized ABBA.
2. We analyze the extra approximation error arising from quantization by relating the computed sum of squared errors to the quantization error, and justify the usage of quantization in QABBA. We believe the insights from our error analysis can also be extended to other quantization methods in deep learning, i.e., quantization-aware training.
3. We investigate large language models with QABBA in time series regression, which showcases the power of symbolic time series representation with language models.
4. We empirically evaluate QABBA compared with other state-of-the-art approaches, using a number of commonly-used datasets, in terms of the approximation error from quantization for different bit lengths and reconstruction quality.

The organization of the paper is as follows. Section 2 gives a brief review of symbolic representation methods. In Section 3, we first formulate the ABBA method to unify the newly introduced notation and explore the potential for the use of quantization within the symbolic approximation of QABBA. Section 4 offers insight into the storage efficiency of ABBA, fABBA, and QABBA. Section 5 showcases the empirical results of competing algorithms across various well-recognized datasets and Section 6 concludes the paper.

## 2 Related work

This section will briefly review some well-established methods for symbolic time series representation with dimensionality reduction as well as their applications. Due to the large a pool of literature in symbolic time series methods, we only illustrate a few of the most popular approaches that achieve dimensionality reduction.

SAX [9] laid the first stone of employing symbolic representation with reduced dimensionality in numerous downstream time series mining tasks, since it enables efficient indexing with a lower-bounding distance measure. SAX uses piecewise aggregate approximation [8] to divide continuous time series into even baskets, and the baskets can be referred to as a representation with reduced dimensionality, denoted as a PAA representation. SAX then converts the PAA representation into a symbolic representation. SAX-related time series mining methods have achieved significant success, e.g., in clustering (SAX Navigator [26], pattern search (SAXRegEx [27]), SPF [28]), anomaly detection (HOT SAX [29], TARZAN [30]) and time series classification (SAX-VSM [31], BOPF [32], MrSQM [15]). Numerous variants of SAX have been proposed to improve performance, e.g., 1d-SAX [10], pSAX [33], cSAX [33]. Their novelty is mainly focused on reconstruction accuracy, but SAX is still a dominant symbolic representation method due to its appealing simplicity and speed.

Compared to SAX, ABBA symbolic approximation [11] achieves better reconstruction and pattern recognition for time series. It relies on adaptive polygonal chain approximation followed by clustering to achieve the symbolization of time series. The reconstruction error of the representation can be modeled as a random walk with pinned start and end points, i.e., a *Brownian bridge*. fABBA [12], a variant of ABBA, uses a computationally efficient greedy aggregation (GA) method to speed up digitization by order of magnitude. Both ABBA and fABBA have been empirically demonstrated to better preserve the shape of time series against SAX, especially the ups and downs behavior of time series. The application of ABBA has been shown to be effective regarding time series prediction and anomaly detection; e.g., the LSTM with ABBA shows robust performance over inference [16], and TARZAN with SAX replaced by ABBA or fABBA compares favorably with SAX-based TARZAN [11, 12]. A downside of ABBA and fABBA is that they are unable to convert multiple time series in a symbolically unified manner. Recent work [34] addresses this issue by introducing a joint representation that enables a consistent symbolization.

### 3 Methodology

In this section, we will briefly recap the ABBA method and establish some notation for the QABBA method which we will use throughout the rest of the paper. As mentioned before, ABBA is an efficient symbolic time series representation method based on an adaptive polygonal chain approximation followed by a means-based clustering algorithm. ABBA symbolization contains two main steps, namely *compression* and *digitization*, to aggregate a time series  $T = [t_1, t_2, \dots, t_n] \in \mathbb{R}^n$  into a symbolic representation  $A = [a_1, a_2, \dots, a_N] \in \mathcal{L}^N$  where  $\mathcal{L}$  denotes a finite alphabet set. A meaningful symbolic representation often has  $N \ll n$ . The reconstruction error is measured by the distance between the original time series  $T$  and the reconstructed time series  $\hat{T}$ . It is evident that a bad symbolic approximation often leads to a high reconstruction error.

Our approach, QABBA, shares a similar procedure with ABBA, but with a quantization step inside the transform, which enables reduced storage space for time series representation. The complete summary of notation for the QABBA procedure is listed in Table 1. The procedures of *symbolization* (the first three steps) and *inverse-symbolization* (the last three steps)<sup>1</sup> are shared among ABBA and QABBA. QABBA contains two additional steps, quantization and inverse-quantization, which can potentially add to the reconstruction error. Note that in the table we use the term “rounding” for the seventh step instead of “quantization” as was used in [11] to avoid confusion.

#### 3.1 Compression

In ABBA, compression is done by computing an adaptive piecewise linear continuous approximation of  $T$  to obtain time series pieces  $P = [(\text{len}_1, \text{inc}_1), \dots, (\text{len}_N, \text{inc}_N)] \in \mathbb{R}^{N \times 2}$ . The ABBA compression plays a central

---

<sup>1</sup>For naming convenience, we define  $\widehat{\text{inc}} = \widetilde{\text{inc}}$ , following [11].

**Table 1** Summary of the QABBA procedure

time series	$T = [t_0, t_1, \dots, t_n] \in \mathbb{R}^n$
after compression	$P = [(\mathbf{len}_1, \mathbf{inc}_1), \dots, (\mathbf{len}_N, \mathbf{inc}_N)] \in \mathbb{R}^{2 \times N}$
after digitization	$A = [a_1, \dots, a_N] \in \mathcal{L}^N, C = [c_1, \dots, c_k] \in \mathbb{R}^{2 \times k}$
after quantization	$A = [a_1, \dots, a_N] \in \mathcal{L}^N, \tilde{C} = [\tilde{c}_1, \dots, \tilde{c}_k] \in \mathbb{N}^{2 \times k}$
inverse-quantization	$A = [a_1, \dots, a_N] \in \mathcal{L}^N, \hat{C} = [\hat{c}_1, \dots, \hat{c}_k] \in \mathbb{R}^{2 \times k}$
inverse-digitization	$\tilde{P} = [(\widetilde{\mathbf{len}}_1, \widetilde{\mathbf{inc}}_1), \dots, (\widetilde{\mathbf{len}}_N, \widetilde{\mathbf{inc}}_N)] \in \mathbb{R}^{2 \times N}$
rounding	$\hat{P} = [(\widehat{\mathbf{len}}_1, \widehat{\mathbf{inc}}_1), \dots, (\widehat{\mathbf{len}}_N, \widehat{\mathbf{inc}}_N)] \in \mathbb{R}^{2 \times N}$
inverse-compression	$\hat{T} = [\hat{t}_1, \hat{t}_2, \dots, \hat{t}_n] \in \mathbb{R}^n$

role in dimensionality reduction in ABBA symbolic approximation—a user-specific tolerance is set to control the degree of the reduction.

The ABBA compression proceeds by adaptively selecting  $N + 1$  indices  $i_0 = 0 < i_1 < \dots < i_N = n$  given a tolerance  $\mathbf{tol}$  such that the time series  $T$  is well approximated by a polygonal chain going through the points  $(i_j, t_{i_j})$  for  $j = 0, 1, \dots, N$ . This results in a partition of  $T$  into  $N$  pieces  $p_j = (\mathbf{len}_j, \mathbf{inc}_j)$  that is determined by  $T_{i_{j-1}:i_j} = [t_{i_{j-1}}, t_{i_{j-1}+1}, \dots, t_{i_j}]$ , each of integer length  $\mathbf{len}_j := i_j - i_{j-1} \geq 1$  in the time direction. Visually, each piece  $p_j$  is represented by a straight line connecting the endpoint values  $t_{i_{j-1}}$  and  $t_{i_j}$ . This partitioning criterion is the squared Euclidean distance of the values in  $p_j$  from the straight polygonal line is upper bounded by  $(\mathbf{len}_j - 1) \cdot \mathbf{tol}^2$ . For simplicity, given an index  $i_{j-1}$  and starting with  $i_0 = 0$ , the procedure seeks the largest possible  $i_j$  such that  $i_{j-1} < i_j \leq n$  and

$$\sum_{i=i_{j-1}}^{i_j} \left( t_{i_{j-1}} + (t_{i_j} - t_{i_{j-1}}) \cdot \frac{i - i_{j-1}}{i_j - i_{j-1}} - t_i \right)^2 \leq (i_j - i_{j-1} - 1) \cdot \mathbf{tol}^2. \quad (1)$$

Each linear piece  $p_j$  of the resulting polygonal chain is a tuple  $(\mathbf{len}_j, \mathbf{inc}_j)$ , where  $\mathbf{inc}_j = t_{i_j} - t_{i_{j-1}}$  is the increment in value, i.e., the subtraction of ending and starting value of  $T_{i_{j-1}:i_j}$ . The whole polygonal chain can be recovered exactly from the first value  $t_0$  and the tuple sequence  $p_1, p_2, \dots, p_N$  where  $p_i = (\mathbf{len}_i, \mathbf{inc}_i) \in \mathbb{R}^2$ . The reconstruction error of this representation is with pinned start and end points and can be naturally modeled as a Brownian bridge. In terms of (1), a lower compression tolerance value  $\mathbf{tol}$  is required to ensure a reasonable recovery error for the compression of time series with a great variety of features, e.g., trends, seasonal and nonseasonal cycles, pulses, and steps.

### 3.2 Digitization

The compression is followed by a digitization that leads to a *symbolic representation*  $A = [a_1, a_2, \dots, a_N] \in \mathcal{L}^N$ ,  $N \ll n$ , and each  $a_j$  is an element of a finite alphabet set  $\mathcal{L}$  where  $|\mathcal{L}| \ll N$ .  $\mathcal{L}$  can be referred to as a dictionary in the ABBA procedure.

Prior to digitizing, a normalization step is applied as indicated [11]; the lengths and increments are separately normalized by the factors  $\sigma_{\text{len}}$  and  $\sigma_{\text{inc}}$ , respectively. The factors  $\sigma_{\text{len}}$  and  $\sigma_{\text{inc}}$  could be standard deviation, or certain scaling so as to map  $\text{len}$  and  $\text{inc}$  to specific range like  $[-1, 1]$ . Following normalization, a parameter  $\text{scl}$  is employed to assign different weights to the length of each piece  $p_i$ , which denotes importance assigned to its length value related to its increment value. Hence, the clustering is effectively computed on

$$\left( \text{scl} \frac{\text{len}_1}{\sigma_{\text{len}}}, \frac{\text{inc}_1}{\sigma_{\text{inc}}} \right), \left( \text{scl} \frac{\text{len}_2}{\sigma_{\text{len}}}, \frac{\text{inc}_2}{\sigma_{\text{inc}}} \right), \dots, \left( \text{scl} \frac{\text{len}_N}{\sigma_{\text{len}}}, \frac{\text{inc}_N}{\sigma_{\text{inc}}} \right). \quad (2)$$

In particular, if  $\text{scl} = 0$ , then clustering will be only performed on the increment values of  $P$ , while if  $\text{scl} = 1$ , the lengths and increments are clustered with equal importance.

The steps after normalization work with vector quantization (VQ); VQ serves as a lossy data compression technique that projects data into a low dimensional space, which has an important role in signal processing. Classical VQ is often achieved by means-based clustering. For ABBA symbolic approximation, Euclidean space is often assumed, which results in the Euclidean clustering problem. The notions of vector quantization are further explained in, e.g., [35, 36]. Given an input of  $N$  vectors  $P = [p_1, \dots, p_N] \in \mathbb{R}^{\ell \times N}$  where  $\ell$  denotes dimensionality (in our context,  $\ell = 2$ ), VQ seeks a codebook of  $k$  vectors, i.e.,  $C = [c_1, \dots, c_k] \in \mathbb{R}^{\ell \times k}$  such that  $k$  is much smaller than  $N$ , where each  $c_i$  is associated with a unique cluster  $S_i$ . A quality codebook enables the sum of squared errors (SSE) to be small enough to an optimal level. Suppose  $k$  clusters  $S_1, S_2, \dots, S_k \subseteq P$  are computed. VQ aims to minimize

$$\text{SSE} = \sum_{i=1}^k \phi(c_i, S_i) = \sum_{i=1}^k \sum_{p \in S_i} \|p - c_i\|_2^2, \quad (3)$$

where  $\phi$  denotes the energy function and  $c_i$  denotes the center of cluster  $S_i$ . We often compute the mean center  $c_i = \frac{1}{|S_i|} \sum_{p \in S_i} p$  for the convergence of the energy function. The k-means algorithm [37] is a suboptimal solution to minimize SSE, i.e., to find  $k$  cluster centers within the data in  $\ell$ -dimensional space to minimize (3). However, solving this problem exactly is NP-hard even if  $k$  is restricted to 2 [38] or in the plane [39]. An alternative solution, used by the fABBA variant, is to use greedy aggregation (GA) [12] which gives an upper bound of  $\alpha^2(N - k)$  for the SSE, where  $\alpha$  is a hyper-parameter as described in [12].

The ABBA digitization can be performed by a suitable partitional clustering algorithm that finds  $k$  clusters from  $P \in \mathbb{R}^{2 \times N}$  such that the SSE given by  $C$  is minimized. The obtained codebook vectors are known as cluster centers. In the context of symbolic approximation, we refer to the cluster centers as *symbolic centers*. Each symbolic center is associated with an identical symbol and each time series snippet  $p_i$  is assigned

with the closest symbolic center  $c^i$  associated with its symbol

$$c^i = \arg \min_{c \in C} (\|p - c\|). \quad (4)$$

Correspondingly each symbolic center is projected to a symbol, written as  $I_d : C \rightarrow A$ . More formally, we define the digitization mapping  $\psi : P \rightarrow A$  as

$$\psi(p_i) = I_d(c^i) = I_d(\arg \min_{c \in C} (\|p - c\|)). \quad (5)$$

Therefore, we can also say each symbol is then associated with a unique cluster (membership). In applications, each clustering label (membership) corresponds to a unique byte-size integer value. The symbols used in ABBA can be represented by text characters, which are not limited to English alphabet letters—often more clusters will be used. Each character in most computer systems is represented by ASCII strings with a unique byte-size integer value (a unique cluster membership). Moreover, it can be any combination of symbols, or ASCII representations. To speedup the digitization, existing work [12] uses GA to replace VQ, which results in a minor loss of approximation accuracy. As analyzed in [12], not all clustering approaches (see e.g., spectral clustering [40], DBSCAN [41] and HDBSCAN [42]) are suitable for the clustering in the digitization phase. This is particularly the case for density clustering methods, which often result in insufficient symbolic information required to fully capture time series patterns, since density clustering methods suffer from the chaining effect and are less likely to result in satisfying SSE, thus leading to high reconstruction error. In this paper, the performance of QABBA in regards to VQ and GA is investigated. However, some parallel implementations might bring potential speed improvement, e.g., parallel k-means [43]. In addition, some methods like CNAK [44] may assist the selection of the  $k$  parameter in ABBA by providing prior knowledge on the number of clusters (distinct symbols).

### 3.3 Quantization and inverse-quantization

In the following, we will formulate the quantization methods and also demonstrate that the usage of quantization in ABBA method introduces an acceptable errors without compromising its reconstruction accuracy. The *quantization* is dominated by three parameters, namely the scale factor  $s \in \mathbb{R}^+$ , the zero-point  $z \in \mathbb{N}$ , and the bit-width  $\omega$ . A quantization mapping  $Q : \mathbb{R} \rightarrow \mathbb{N}$  aims to map a floating point number  $x \in [\zeta, \eta]$  to a  $\omega$ -bit integer  $\tilde{x} \in [\tilde{\zeta}, \tilde{\eta}]$ . The bit-width  $\omega$  is used to compute the range of  $\tilde{x}$ ; often, we apply  $\tilde{\zeta} = -2^{\omega-1}$  and  $\tilde{\eta} = 2^{\omega-1} - 1$ . The quantization mapping is given by

$$\tilde{x} = Q(x) = \lfloor \frac{1}{s}x - z \rfloor, \quad (6)$$

where  $s = \frac{\eta - \zeta}{\tilde{\eta} - \tilde{\zeta}}$ , and  $\lfloor \cdot \rfloor$  is the operator that rounds the value to the nearest integer.

Often, a clipping is employed for the quantized value, that is,

$$\text{clip}(x, a, b) = \begin{cases} a & \text{if } x < a \\ x & \text{if } a \leq x \leq b \\ b & \text{if } x > b \end{cases}.$$

Hence (6) will become

$$\tilde{x} = Q(x) = \text{clip}(\lfloor \frac{1}{s}x - z \rfloor, a, b). \quad (7)$$

If  $a, b$  are exactly  $\tilde{\zeta}, \tilde{\eta}$ , respectively, the clip operation can be omitted. Accordingly, the *inverse-quantization* is defined as

$$y = Q^{-1}(\tilde{x}) = s(\tilde{x} + z) = s(\text{clip}(\lfloor \frac{1}{s}x - z \rfloor, a, b) + z). \quad (8)$$

It is worth noting that when the zero-point  $z$  is set to zero, the quantization degrades to a case of particular interest, called symmetric quantization, which avoids additional overheads of handling zero-point offset [45], and naturally results in smaller quantization error and SSE.

Accordingly, the symbolic centers  $C$  are quantized as  $\tilde{C} := Q(C)$  where  $\tilde{c}_{ij} = Q(c_{ij})$ . For the reconstruction of the symbolic representation, we simply inverse-quantize  $\tilde{C}$  to obtain  $\hat{C}$  by (8). As a consequence, the reconstruction error for QABBA can potentially be increased. Given the precision  $\delta$  of the quantized value, we will assume that there is no rounding error arising from floating pointing arithmetic. This is a valid assumption since the rounding error will be dominated by the operation  $\lfloor \cdot \rfloor$  (i.e., the working precision  $u \ll \delta$ ). Omitting the clip operation, we therefore assume the following model:

$$\lfloor f \rfloor = f + \delta, \quad |\delta| \leq \frac{\tilde{\eta} - \tilde{\zeta}}{2^{\omega+1} - 2}. \quad (9)$$

Thus, (6) can be written as

$$\tilde{x} = \frac{1}{s}x - z + \delta, \quad |\delta| \leq \frac{\tilde{\eta} - \tilde{\zeta}}{2^{\omega+1} - 2}. \quad (10)$$

By plugging this into (8), we obtain,

$$y = Q^{-1}(\tilde{x}) = x + s\delta = x + \frac{\eta - \zeta}{2^{\omega+1} - 2}, \quad (11)$$

which shows the errors arising from quantization only relate to  $\zeta, \eta$ , and  $\omega$ .

Accordingly, given  $C = [c_1, \dots, c_k] \in \mathbb{R}^{2 \times k}$ , the error from the quantization in terms of the Frobenius norm is

$$\|\tilde{C} - C\|_F \leq \frac{\eta - \zeta}{2^{\omega+1} - 2} \|E\|_F = \frac{\sqrt{2k}(\eta - \zeta)}{2^{\omega+1} - 2}, \quad (12)$$



where  $E$  is the 2 by  $k$  matrix of ones.

The new quantized SSE computed by the mean center  $c_i = \sum_{p \in S_i} p / |S_i|$  is upper bounded by

$$\begin{aligned} \widehat{\text{SSE}} &= \sum_{i=1}^k \sum_{p \in S_i} \|p - \tilde{c}_i\|_2^2 = \sum_{i=1}^k \sum_{p \in S_i} \left( \|p - c_i\|_2^2 + \|c_i - \tilde{c}_i\|_2^2 \right) \\ &= \sum_{i=1}^k \left( \sum_{p \in S_i} \|p - c_i\|_2^2 + |S_i| \|c_i - \tilde{c}_i\|_2^2 \right) \\ &\leq \text{SSE} + \frac{2N(\eta - \zeta)^2}{(2^{\omega+1} - 2)^2}, \end{aligned} \quad (13)$$

where  $|\cdot|$  indicates cardinality of the set. Note that the first equality holds because

$$\sum_{p \in S_i} 2(p - c_i)^T (c_i - \tilde{c}_i) = (c_i - \tilde{c}_i)^T \sum_{p \in S_i} 2(p - c_i) = 0$$

since  $c_i = \frac{\sum_{p \in S_i} p}{|S_i|}$ .

With respect to the QABBA context and assuming, e.g., a min-max normalization is employed, i.e.,  $\sigma_{\text{len}} := \max(\text{len}) - \min(\text{len})$  and  $\sigma_{\text{inc}} := \max(\text{inc}) - \min(\text{inc})$ , then the values of  $P$  is scaled to a specific range  $[-1, 1]$ . As such, following (13), the upper bound of the term  $\frac{2N(\eta - \zeta)^2}{(2^{\omega+1} - 2)^2}$  will become negligible compared to the size of SSE itself since  $\frac{(\eta - \zeta)^2}{(2^{\omega+1} - 2)^2} \ll 1$ .

### 3.4 Symbolic reconstruction

The *symbolic reconstruction* (also called *inverse symbolization*) refers to converting the symbolic representation  $A$  into the reconstructed series  $\hat{T}$  such that the distance between  $\hat{T}$  and  $T$  is minimized—the error arising from symbolic approximation—is reasonably small. The symbolic reconstruction contains four dominant steps. First, we inverse quantize the integer type symbolic centers  $\tilde{C}$ . Second, the *inverse-digitization* is computed, simply written as  $\psi^{-1}$  (see Equation (5)), which uses the  $k$  representative elements  $c_i \in C$  (in terms of, e.g., mean centers or median center of the groups  $S$ ) to separately replace the symbols in  $A$ , and thus results in a 2-by- $N$  array  $\tilde{P}$ , i.e., an approximation of  $P$ , where each  $\tilde{p}_i \in \tilde{P}$  is the closest symbolic center  $c^i \in C$  to  $p_i \in P$ .

The inverse digitization often leads to a non-integer value for the reconstructed length  $\text{len}$ , so [11] proposes a novel rounding method to align the cumulated lengths with the closest integers, which is the third step. We round the first length to an integer value, i.e.,  $\widehat{\text{len}}_1 := \text{round}(\text{len}_1)$  and calculate the rounding error  $e := \text{len}_1 - \widehat{\text{len}}_1$ . The error is then added to the rounding of  $\text{len}_2$ , i.e.,  $\widehat{\text{len}}_2 := \text{round}(\widehat{\text{len}}_1 + e)$ , and the new error  $e'$  is calculated as  $\widehat{\text{len}}_2 + e - \text{len}_2$ . Then  $e'$  is involved in the next rounding similarly. After all rounding is computed, we obtain

$$\hat{P} = [(\widehat{\text{len}}_1, \widehat{\text{inc}}_1), \dots, (\widehat{\text{len}}_N, \widehat{\text{inc}}_N)] \in \mathbb{R}^{2 \times N}, \quad (14)$$

where the increments  $\mathbf{inc}$  are unchanged, i.e.,  $\widehat{\mathbf{inc}} = \widetilde{\mathbf{inc}}$ . The last step is to recover the whole polygonal chain exactly from the initial time value  $t_0$  and the tuple sequence (14) via the inverse compression.

A more intuitive understanding of the symbolic approximation via QABBA can be obtained from Fig. 1, which shows three ECG (Electrocardiogram) signals reconstructed using the QABBA (VQ & GA) symbolic approximation associated with an 8-bit quantization for length and 16-bit quantization for increment, using  $\mathbf{tol} = 0.1$  and  $\alpha = 0.4$ . We observe that the reconstructed data (for the first and second signals) via QABBA (GA) with  $\mathbf{scl} = 1$  has a shift in the x-horizon. This can be fixed by using a higher  $\mathbf{scl}$  value, e.g.,  $\mathbf{scl} = 5$ , as illustrated in Fig. 1. Table 2 lists the parameter settings, symbolic representation (output), as well as the number of distinct symbols ( $\#Symbols$ ) used for the three signals.

The inverse symbolization of ABBA unavoidably leads to some reconstruction errors due to the limited parameter space. Note that the reconstruction error is equivalent to the approximation error of the ABBA symbolization. The reconstruction error can be quantified via the mean squared error (MSE), which is given by

$$\text{MSE} = \frac{1}{i} \sum_i^n (t_i - \hat{t}_n)^2, \quad (15)$$

and its square root is referred to as root mean square error (RMSE).

Other approaches including Euclidean distance, Dynamic time warping (DTW) [46], as well as the differenced ones used in [11] can also provide insights into the approximation error. For the purpose of comprehensive evaluation, we use a combination of them in this paper.

**Table 2** Symbolic approximation of ECG signals.

Signals	Parameter setting	Symbolic representation	$\#Symbols$	MSE
I	QABBA (VQ, scl=1)	AceDfCBdabEaGF	13	0.12
	QABBA (GA, scl=1)	ABCeDfGFEbdDca	13	0.058
	QABBA (VQ, scl=5)	AcFGDaECeddBfg	14	0.058
	QABBA (GA, scl=5)	baBcCGgfEeFdDA	14	0.058
II	QABBA (VQ, scl=1)	AbdCDBEacECbeFfA	12	0.32
	QABBA (GA, scl=1)	AbeEFfdDadcbBCcA	12	0.073
	QABBA (VQ, scl=5)	AHFECagdDbcBfeGA	15	0.069
	QABBA (GA, scl=5)	ACEdgHGeFfeDbABA	15	0.12
III	QABBA (VQ, scl=1)	ADCadcBeEbdC	10	0.29
	QABBA (GA, scl=1)	AabdcEeCBDcb	10	0.12
	QABBA (VQ, scl=5)	AEcdbBaeCDbc	10	0.069
	QABBA (GA, scl=5)	aBAbCEecDdCA	10	0.12

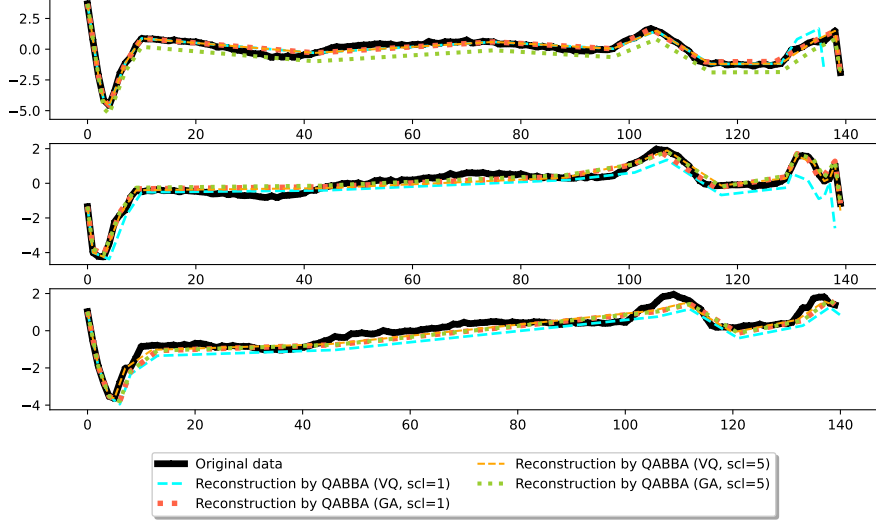


**Fig. 1** Reconstructed ECG signals from QABBA symbolic approximation.

## 4 Storage efficiency

As discussed previously, the ABBA method and its variants are symbolic approximation techniques that achieve efficient data compression, significantly reducing the storage need of time series. It is known that reconstructing an ABBA representation requires the initial value(s), symbolic center(s), and strings (we refer to Section 3 for more detail). Therefore, to store the time series representation, only these three variables are needed.

Time series are often represented as floating point numbers, primarily 32 bits, i.e., single-precision format (abbreviated as float32). To store the time series, we require  $B_T$  bits for each value. The character data type for strings requires 8 bits. Let's assume  $B_{len}$  and  $B_{inc}$  bits are used to represent each `len` and `inc` value of the symbolic centers of length  $k$ , respectively. The dominant storage of ABBA symbolic representation associated with  $p$  initial values thus requires  $8N + (B_{len} + B_{inc}) \cdot k + p \cdot B_T$  bits. The compression ratio of a time series (of length  $n$ ) is defined as the ratio between the uncompressed size and compressed size, which is given by

$$\varphi_{ABBA} = \frac{8N + (B_{len} + B_{inc}) \cdot k + p \cdot B_T}{B_T \cdot n}. \quad (16)$$

For ABBA approximation, if float32 is used for the time series and all values of symbolic centers, then (16) can be computed as  $\varphi_{ABBA} = \frac{8N+64k+32}{32n}$ , which also holds for the fABBA variant.

Compared to ABBA, QABBA requires additional storage for the parameters  $s$  and  $z$ , which use the  $B_s$  bits for each; the additional storage is constant complexity, and

thus won't significantly affect the compression ratio. The compression ratio  $\varphi_{QABBA}$  can similarly be formulated as

$$\varphi_{QABBA} = \frac{8N + (B_{\text{len}} + B_{\text{inc}}) \cdot k + p \cdot B_T + 2B_s}{B_T \cdot n}. \quad (17)$$

If we use  $p = 1$ ,  $B_T = 32$ ,  $B_{\text{len}} = 8$ ,  $B_{\text{inc}} = 12$ , and  $B_s = 32$  for (17), then we have  $\varphi_{QABBA} = \frac{8N + 20 \cdot k + 96}{32 \cdot n}$ .

As explained in (16) and (17), the compression ratio of the ABBA representation relies on  $N$ ,  $k$ , and  $n$  which are manageable by tuning the hyperparameters `tol`,  $k$ , and  $\alpha$  to obtain an acceptable approximation error. The storage efficiency of QABBA over ABBA originates from using lower bit-width to decrease  $B_{\text{len}}$  and  $B_{\text{inc}}$  such that the reliance on  $k$  is minimized. The required storage for symbolic approximation resulting from QABBA and ABBA relies heavily on the size of symbolic centers  $C$  and the length of the symbolic representation, i.e.,  $N$ .

## 5 Empirical Results

In this section, we compare the performance of non-quantized ABBA, i.e., ABBA and fABBA, quantized ABBA, and SAX-based algorithms, in terms of storage and approximation errors. We conduct extensive experiments on synthetic time series as well as and well-established real-world datasets including those from the UCR Archive [47] and the UEA Archive [48]. To ensure a fair comparison, we selected competing algorithms with publicly available software implementations.<sup>2</sup> Our software is integrated into the established fABBA library (<https://github.com/nla-group/fABBA>), and the experimental code is openly available at:

<https://github.com/inEXASCALE/qabba>.

In the following experiments, we compare QABBA with ABBA, fABBA, SAX, and 1d-SAX algorithms. Additionally, we test two variants of QABBA—QABBA (VQ) and QABBA (GA)—which use `k-means++` [49] and greedy aggregation [12], respectively, in the digitization stage. All experiments here except Section 5.2 are simulated in Python on a Dell PowerEdge R740 Server with Intel Xeon Silver @ 4114 2.2GHz and 1.5 TB RAM.

### 5.1 Approximation error from quantization

To evaluate QABBA, it is critical to understand how the number of bits used affects the performance of symbolic approximation. In this experiment, we evaluate the performance of QABBA in terms of the number of bits used to store the lengths and increments. The experimental data are 100 synthetic time series of length 5,000 generated using a standard normal Gaussian distribution. For QABBA, we quantize either `len` or `inc` to a lower bit-width integer format while fixing the other to float32 format.

---

<sup>2</sup>ABBA and fABBA are accessible at <https://github.com/nla-group/ABBA> and <https://github.com/nla-group/fABBA>, respectively.

The approximation error is evaluated in terms of the MSE ((15)) distance between the original time series and the reconstructed time series.

The results are depicted in Fig. 2. We can see that the error arising from quantizing the increment, compared to the `len`, increases dramatically as the bit-width decreases. In other words, the impact of quantizing the `len` values is much less than that of quantizing the `inc` values. The safety margin of the quantization bits for `len` quantization in this dataset is in  $[8, 32]$  whereas for `inc` quantization it is  $[12, 32]$  (for there to be an advantage to quantization, the bit-width should be lower than 32). This provides guidance for choosing the bit-width for the quantizations in practice. All experiments in the following sections will simulate QABBA with a quantization of 8 bits for the `len` values of the symbolic centers and 12 bits for the `inc` values of the symbolic centers.

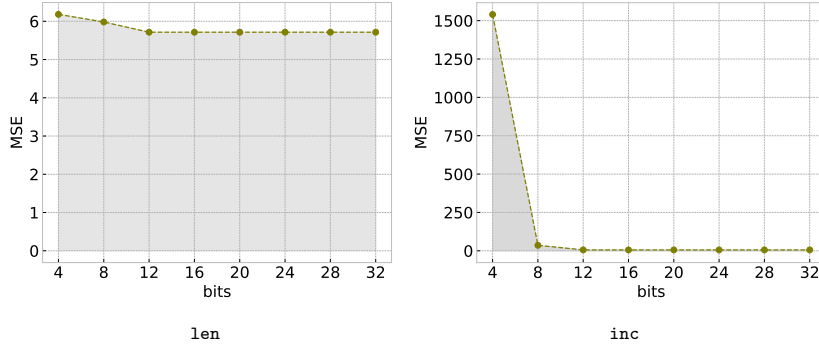


Fig. 2 Reconstruction error arising from quantization.

## 5.2 LLM with QABBA for time series regression

In this section, we show that QABBA can exploit the semantic information hiding beneath the time series in the task of time series regression. For the regression task, we evaluate one pre-trained LLM using the Time Series Extrinsic Regression (TSER) benchmark archive [50], which contains 19 time series datasets from 5 distinct areas, ranging from health monitoring, energy monitoring, environment monitoring, sentiment analysis to forecasting<sup>3</sup>. Details of the hyperparameter settings of our implementation can be found in Table 3. We simulated QABBA in various bit-width settings for `len` and `inc` and applied one commonly-used LLM - Mistral-7B [51] - to tackle time series regression problems. In the first, the numerical time series is transformed to the symbolic series, and the corresponding label is still a number. By replacing the last layer with a regression layer, we fine-tune Mistral-7B on the training data using QLoRA [52] with inhibition [53]. All the experiments are simulated in PyTorch [54] and conducted on a single NVIDIA A100 40GB GPU.

<sup>3</sup>Monash regression data is available at <http://tseregression.org/>.

The empirical results are shown in Table 4, in which 9 out of 16 use-cases outperform the machine learning state-of-the-art results (SOTA). Specifically, when using 16 bit-width for both **len** and **inc**, QABBA not only shows competitive performance for the regression of time series but also occupies less memory space. Also, we can observe that lower bit-width use for **len** and **inc** only does not degrade the performance of regression much. QABBA is able to provide chain-of-patterns to LLMs by compressing and digitizing time series to symbols, which finally results in the change of embedding space by using adaption fine-tuning methods. The benefits of QABBA with LLMs include (1) avoiding the need for LLMs to learn time series from scratch, (2) only utilizing compression and decompression without the need for the training of extra embeddings [55].

**Table 3** Hyperparameters of the time series regression task. Quant. is the LoRA quantization process. Inhib. is the inhibition threshold in QLoRA. MAE is mean absolute error.

QLoRA Hyperparameters					QABBA Hyperparameters				
quant 4-bit	low rank	alpha	inhi.	dropout	inc	len	init	tol	alpha scl
True	16	16	0.3	0.05	16, 32	32, 16, 12, 8	agg	0.001	0.001 3
LLM Hyperparameters									
batch size	learning rate	epochs	max length	optim	weight decay	warmup steps	loss function		
4	2e-4	20	4,096	adamw_8bit	5e-5	5	MAE		

**Table 4** The performance (RMSE: root mean square error) of time series regression task on QABBA. SOTA is the results of [50].

LLM	Quantize			Monash Regression Data						
	len	inc	App.	Hou.1	Hou.2	Ben.	Bei.1	Bei.2	Liv.	Flo.1
Mistral-7B	32	32	2.34	228.83	24.51	4.03	65.24	53.49	20.88	0.36
Mistral-7B	16	16	2.34	228.63	<b>24.51</b>	4.03	<b>65.24</b>	53.49	<b>20.85</b>	0.36
Mistral-7B	12	16	2.34	228.78	24.56	4.03	65.25	<b>53.49</b>	20.88	0.36
Mistral-7B	8	16	2.43	228.83	24.54	4.03	65.25	53.50	20.94	0.37
SOTA	-	-	<b>2.29</b>	<b>132.80</b>	32.61	<b>0.64</b>	93.14	59.50	28.80	<b>0.00</b>

LLM	Quantize			Monash Regression Data						
	len	inc	Flo.2	Flo.3	Aus	PPG	IEE.	Ne.H	Ne.T	Cov.
Mistral-7B	32	32	0.39	0.39	5.89	12.58	23.03	0.10	0.10	0.03
Mistral-7B	16	16	0.39	0.37	<b>5.89</b>	12.58	<b>23.02</b>	<b>0.10</b>	0.10	0.03
Mistral-7B	12	16	0.39	0.39	5.90	12.61	23.05	0.11	<b>0.10</b>	0.03
Mistral-7B	8	16	0.40	0.41	5.92	12.62	23.08	0.12	0.11	<b>0.03</b>
SOTA	-	-	<b>0.01</b>	<b>0.00</b>	8.12	<b>9.92</b>	23.90	0.14	0.14	0.04

### 5.3 Performance profiles in UCR Archive

The concept of *performance profiles* [56] has been introduced as an efficient benchmarking tool for evaluating the performance of a set of optimization algorithms over a large set of test problems. It has been verified that performance profiles can handle the influence of a small number of problems for evaluation and are less sensitive to the results affiliated with the ranking of algorithms.

The performance profile for an algorithm is represented by the cumulative distribution function (CDF) for a performance measure. Let  $\mathcal{V}$  be a set of problems and let  $\mathcal{S}$  be a set of algorithms. The quantity  $s_{i,j} \geq 0$  denotes a performance measurement of algorithm  $i \in \mathcal{S}$  run on problem  $j \in \mathcal{V}$ , assuming that a smaller value of  $s_{i,j}$  is better. For any problem  $j \in \mathcal{V}$ , let  $\hat{s}_j = \min\{s_{i,j} : i \in \mathcal{S}\}$  be the best performance of an algorithm on problem  $j$ . The performance ratio  $r_{i,j}$  is given by

$$r_{i,j} = \frac{s_{i,j}}{\hat{s}_j}, \quad (18)$$

where  $r_{i,j} = 0$  indicates that algorithm  $i$  fails on problem  $j$ . We define

$$\xi(r_{i,j}, \theta) = \begin{cases} 1 & \text{if } r_{i,j} < \theta \\ 0 & \text{otherwise} \end{cases} \quad (19)$$

where  $\theta \geq 1$ . The *performance profile of solver  $i$*  is

$$\rho_i(\theta) = \frac{\sum_{j \in \mathcal{V}} \xi(r_{i,j}, \theta)}{|\mathcal{V}|}, \quad \theta \geq 1. \quad (20)$$

From a statistics perspective,  $\rho_i(\theta)$  can be regarded as the empirical probability that the performance ratio  $r_{i,j}$  for algorithm  $i \in \mathcal{S}$  and each problem  $j \in \mathcal{V}$  is within a factor  $\theta$  of the best possible ratio. The graph of the CDF  $\rho_i$ —the performance profile—reveals several features in a visually convenient way, e.g., a line which more closely approaches the upper left corner indicates a better algorithm. In particular, algorithms  $i$  with fast-increasing performance profiles are preferable if the problem set  $\mathcal{V}$  is suitably large and representative of problems likely to occur in applications.

The setting of the first experiment follows [11]. In this simulation, we evaluate SAX, 1d-SAX, ABBA, fABBA, and QABBA (VQ & GA) across all datasets (a total of 201,161 time series) in the UCR Archive. The experimental design follows [12]; we first run fABBA with a given digitization rate  $\alpha$ , and then take the number of distinct symbols of the representation as  $k$  and feed the same  $\alpha$  and  $k$  values to other symbolic representation methods for a fair comparison. We evaluate Euclidean distance, DTW distance, and their differenced counterparts to benchmark performance on the UCR Archive data in terms of two different settings of digitization rate. Recall that QABBA variants use 8 bits for the lengths and 12 bits for the increments.

The resulting performance profiles are depicted in Fig. 3 and Fig. 4. First, we observe that QABBA results in a slight loss in terms of reconstruction, and the loss is proportional to  $\alpha$  (i.e., the fewer symbolic centers used, the greater the loss for the QABBA reconstruction). Second, we found that QABBA (VQ) closely follows ABBA in both Fig. 3 and Fig. 4, especially in Fig. 4 with  $\alpha = 0.5$ . Additionally, the runtime of QABBA against ABBA is as shown in Table 5, which shows the quantization introduce

almost no speed loss under ABBA framework. Overall, QABBA exhibits comparable performance regarding reconstruction versus ABBA.

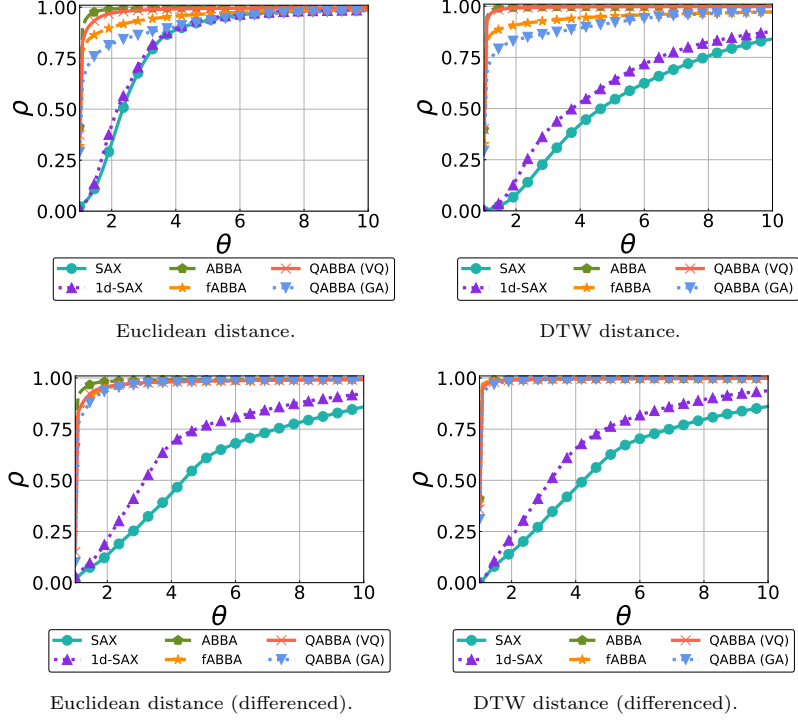


**Fig. 3** Performance profiles ( $\alpha = 0.1$ ).

## 5.4 Simulations in UEA Archive

The UEA Archive contains a wide range of multivariate time series from real-world applications. Directly employing ABBA, fABBA and QABBA (GA & VQ) on these datasets is not possible, since the consistency of symbols is not guaranteed. We use the joint symbolic representation introduced in [34] to enable the computation of symbolic approximations of multivariate time series data in a unified manner.

In this experiment, we evaluate the competing ABBA-based algorithms in terms of approximation error and compression ratio for selected datasets from the UEA Archive (see Table 5). The approximation error is measured by the distance between ground truth data and reconstructed data (simply computed as the average of the squared differences given multidimensional tensor). The compression time is not measured since all algorithms perform the same compression and their differences lie only in their digitization. All algorithms use the same number of symbolic centers. We use the compression ratio defined in Section 4 to evaluate the storage savings. Experiments



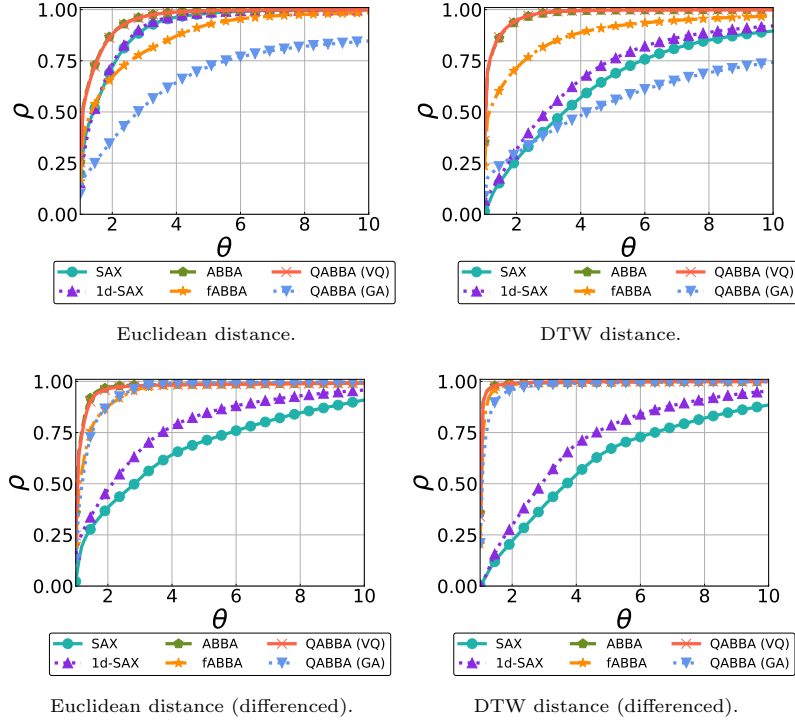


**Fig. 4** Performance profiles ( $\alpha = 0.5$ ).

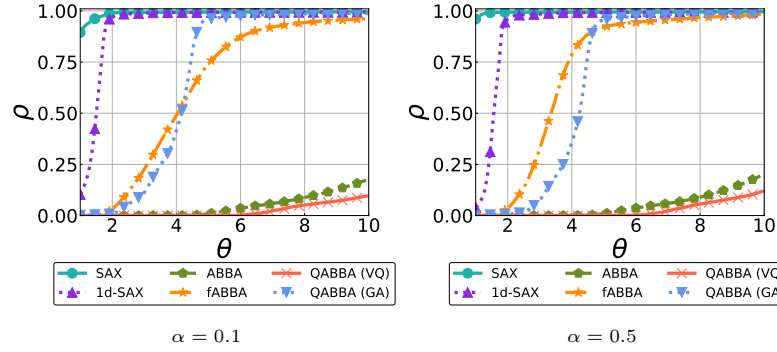


**Fig. 5** Performance profiles in Runtime.

using two compression settings ( $\text{tol} = 0.005$  and  $\text{tol} = 0.05$ ) are shown in Fig. 8 and Fig. 9.

Fig. 9 describes the compression ratio as well as their respective component portions, which shows that the storage savings of QABBA are significant; the needed storage is almost half of that without quantization), and this comes at the cost of negligible increased reconstruction error. Besides, in terms of Fig. 9, it shows that a large

portion of the storage of these methods has been devoted to the strings, therefore, a further significant compression can be obtained from LZW [57].

The approximation error of QABBA compared to the non-quantized variants (e.g., comparing ABBA and QABBA (VQ) and fABBA and QABBA (GA)) remains similar in terms of DTW distance but can be significantly higher in terms of MSE. We can thus conclude that quantization causes more error as measured by MSE than as measured by DTW. We note that our bit-widths for the length and increment values were taken from our experiments with synthetic data; it likely that in practice, one will have to tune these parameters to a specific dataset, which can result in improved reconstruction error.

The acceptable error can be evaluated perceptually by plotting both the raw time series and the reconstruction; if they are close enough, this might be “acceptable”. Both ABBA and fABBA are well-established methods for quality symbolic reconstruction, and our intent is to validate the reconstruction error by comparing it with ABBA or fABBA. Hence we plot the reconstruction of ABBA, fABBA, QABBA (VQ), and QABBA (GA) performed with `tol = 0.05` in the first (others’ performance is similar through our test) multivariate time series of the UEA datasets in Table 5 following the settings described in Section 5.4. The reconstruction comparisons are as shown in Fig. 6 and 6. The reconstruction of ABBA and QABBA almost overlaps with the original time series, which demonstrates that all the tested methods achieve satisfying reconstruction, and the comparison of their storage is justified.

**Table 5** Selected datasets from the UEA Archive.

Dataset	Size	Dimension	Length
AtrialFibrillation	30	2	640
BasicMotions	80	6	100
CharacterTrajectories	2,858	3	182
Epilepsy	275	3	206
JapaneseVowels	640	12	29
NATOPS	360	24	51
UWaveGestureLibrary	440	3	315

## 6 Summary and future work

In this paper, we present a quantization-based symbolic approximation method for time series, called QABBA, and explore its performance regarding reconstruction error and storage efficiency in various datasets. We theoretically and practically validate the possibility and potential of using quantization in ABBA; We investigate the required bit-width for quantization to ensure an acceptable symbolic reconstruction and also contribute a theoretical understanding of the correlation between the quantization error and errors of symbolic approximation, where the analysis can be applicable to other quantization algorithms. The empirical results demonstrate that

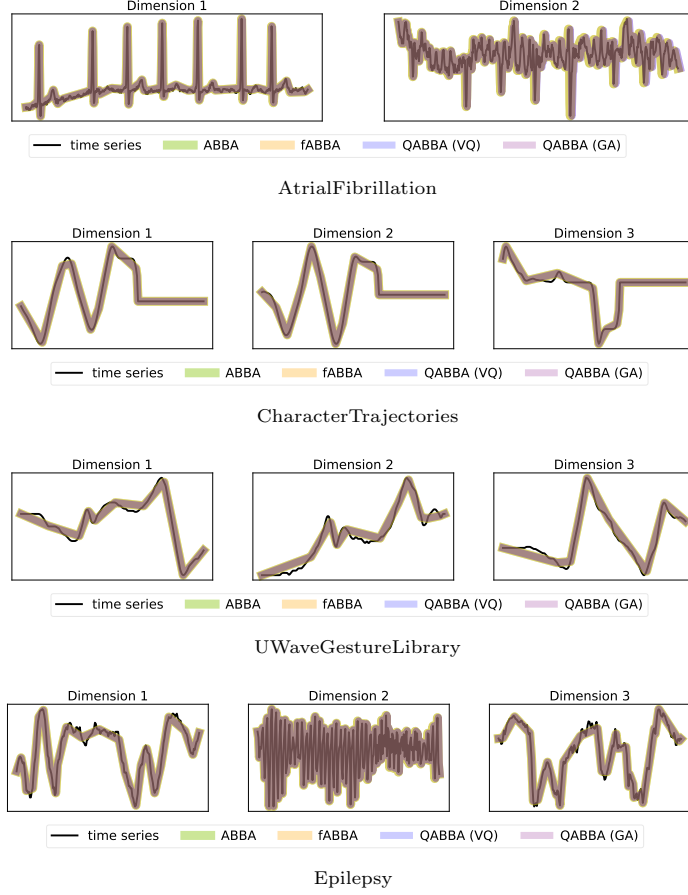


**Fig. 6** Symbolic reconstruction of UEA Archive (I).

QABBA achieves only a fraction of the storage needed for symbolic approximation while maintaining an acceptable accuracy compared with ABBA and fABBA without speed loss. Our application of interest here is not time series compression, we aim to preserve the time series structure and patterns under a further compression, and a further compression can be further obtained from LZW compression. We believe a lower bit-width representation may be promising in certain scenarios. We also investigate the performance of time series regression for QABBA with language models, which demonstrates the potential benefits of our symbolic approximation technique. The semantic understanding of time series using QABBA is promising in many time series mining tasks, and further study will be left as future work.

## Acknowledgements

The first author acknowledges funding from the European Union (ERC, inEXASCALE, 101075632). Views and opinions expressed are those of the authors only and do

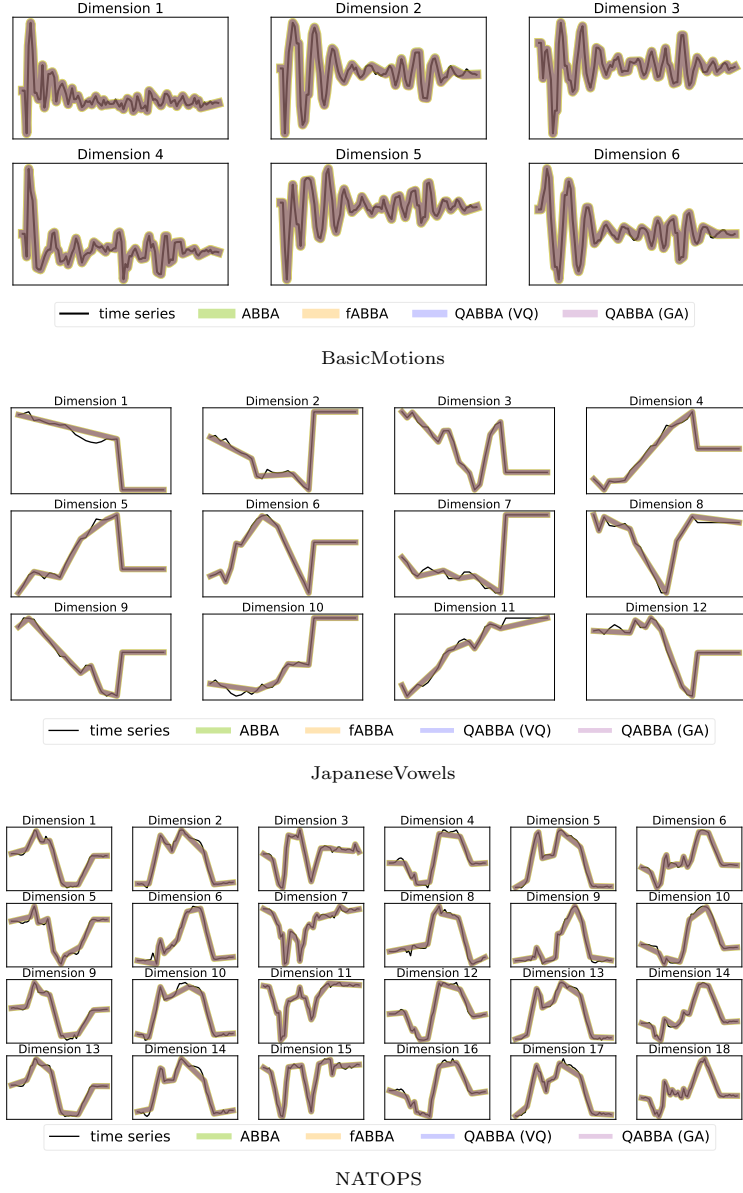


**Fig. 7** Symbolic reconstruction of UEA Archive (II).

not necessarily reflect those of the European Union or the European Research Council. Neither the European Union nor the granting authority can be held responsible for them. Additionally, the first author acknowledges funding from the Charles University Research Centre program (No. UNCE/24/SCI/005). The second author acknowledges funding from the France 2030 NumPEX Exa-MA project (ANR-22-EXNU-0002), managed by the French National Research Agency (ANR).

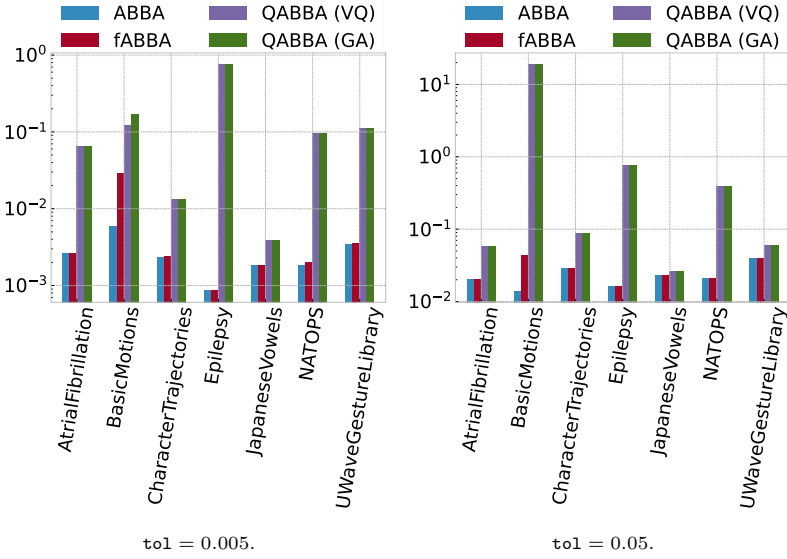


**Fig. 8** Errors of reconstruction.

## References

- [1] Indyk, P., Motwani, R.: Approximate nearest neighbors: Towards removing the curse of dimensionality. In: ACM Symposium on Theory of Computing. STOC '98, pp. 604–613 (1998). <https://doi.org/10.1145/276698.276876>
- [2] Jensen, S., Pedersen, T., Thomsen, C.: Time series management systems: A survey. IEEE Transactions on Knowledge and Data Engineering **29**(11), 2581–2600 (2017) <https://doi.org/10.1109/TKDE.2017.2740932>
- [3] Esling, P., Agon, C.: Time-series data mining. ACM Computing Surveys **45**(1) (2012) <https://doi.org/10.1145/2379776.2379788>
- [4] Chiarot, G., Silvestri, C.: Time series compression survey. ACM Computing Surveys **55**(10) (2023) <https://doi.org/10.1145/3560814>
- [5] Kontaki, M., Papadopoulos, A.N.: Efficient similarity search in streaming time sequences. In: Proceedings of the 16th International Conference on Scientific and Statistical Database Management, pp. 63–72. IEEE, Greece (2004). <https://doi.org/10.1109/SSDM.2004.1311194>
- [6] Assent, I., Wichterich, M., Krieger, R., Kremer, H., Seidl, T.: Anticipatory DTW for efficient similarity search in time series databases. Proceedings of the VLDB Endowment **2**, 826–837 (2009) <https://doi.org/10.14778/1687627.1687721>
- [7] Francis, B., Dasgupta, S.: Signal compression by subband coding. Automatica

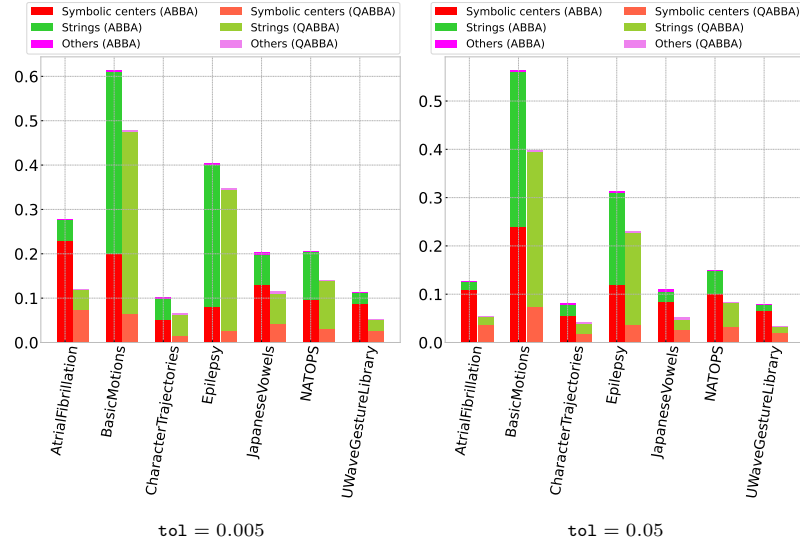


**Fig. 9** Compression ratio.

**35**(12), 1895–1908 (1999) [https://doi.org/10.1016/S0005-1098\(99\)00132-7](https://doi.org/10.1016/S0005-1098(99)00132-7)

- [8] Chakrabarti, K., Keogh, E., Mehrotra, S., Pazzani, M.: Locally adaptive dimensionality reduction for indexing large time series databases. *ACM Transactions on Database Systems* **27**(2), 188–228 (2002) <https://doi.org/10.1145/568518.568520>
- [9] Lin, J., Keogh, E., Lonardi, S., Chiu, B.: A symbolic representation of time series, with implications for streaming algorithms. In: *Proceedings of the 8th ACM SIGMOD Workshop on Research Issues in Data Mining and Knowledge Discovery*, pp. 2–11. ACM, USA (2003). <https://doi.org/10.1145/882082.882086>
- [10] Malinowski, S., Guyet, T., Quiniou, R., Tavenard, R.: 1d-SAX: A novel symbolic representation for time series. In: *Advances in Intelligent Data Analysis XII* (2013). [https://doi.org/10.1007/978-3-642-41398-8\\_24](https://doi.org/10.1007/978-3-642-41398-8_24)
- [11] Elsworth, S., Güttel, S.: ABBA: adaptive Brownian bridge-based symbolic aggregation of time series. *Data Mining and Knowledge Discovery* **34**, 1175–1200 (2020) <https://doi.org/10.1007/s10618-020-00679-8>
- [12] Chen, X., Güttel, S.: An efficient aggregation method for the symbolic representation of temporal data. *ACM Transactions on Knowledge Discovery from Data* (2022) <https://doi.org/10.1145/3532621>
- [13] Lin, J., Keogh, E., Wei, L., Lonardi, S.: Experiencing SAX: a novel symbolic representation of time series. *Data Mining and Knowledge Discovery* **15**(2), 107–144 (2007) <https://doi.org/10.1007/s10618-007-0064-z>

- [14] Senin, P., Lin, J., Wang, X., Oates, T., Gandhi, S., Boedihardjo, A.P., Chen, C., Frankenstein, S.: Time series anomaly discovery with grammar-based compression. In: 18th International Conference on Extending Database Technology, pp. 481–492. OpenProceedings.org, ??? (2015). <https://doi.org/10.5441/002/edbt.2015.43>
- [15] Nguyen, T.L., Ifrim, G.: Fast time series classification with random symbolic subsequences. In: Advanced Analytics and Learning on Temporal Data: 7th ECML PKDD Workshop, AALTD 2022, pp. 50–65. Springer, France (2023). [https://doi.org/10.1007/978-3-031-24378-3\\_4](https://doi.org/10.1007/978-3-031-24378-3_4)
- [16] Elsworth, S., Güttel, S.: Time series forecasting using LSTM networks: A symbolic approach, 12 (2020) [2003.05672](https://doi.org/10.1007/978-3-031-24378-3_4)
- [17] Criado-Ramón, D., Ruiz, L.G.B., Pegalajar, M.C.: Electric demand forecasting with neural networks and symbolic time series representations. Applied Soft Computing **122**, 108871 (2022) <https://doi.org/10.1016/j.asoc.2022.108871>
- [18] Li, Y., Lin, J.: Approximate variable-length time series motif discovery using grammar inference. In: Proceedings of the 10th International Workshop on Multimedia Data Mining. MDMKDD '10. ACM, USA (2010). <https://doi.org/10.1145/1814245.1814255>
- [19] Zhang, S., Bahrapour, S., Ramakrishnan, N., Schott, L., Shah, M.: Deep learning on symbolic representations for large-scale heterogeneous time-series event prediction. In: 2017 IEEE International Conference on Acoustics, Speech and Signal Processing, pp. 5970–5974 (2017). <https://doi.org/10.1109/ICASSP.2017.7953302>
- [20] Tamura, K., Ichimura, T.: Clustering of time series using hybrid symbolic aggregate approximation. In: IEEE Symposium Series on Computational Intelligence, pp. 1–8 (2017). <https://doi.org/10.1109/SSCI.2017.8280846>
- [21] Lee, J., Kim, C., Kang, S., Shin, D., Kim, S., Yoo, H.-J.: UNPU: A 50.6TOPS/W unified deep neural network accelerator with 1b-to-16b fully-variable weight bit-precision. In: IEEE International Solid-State Circuits Conference, pp. 218–220. IEEE, USA (2018). <https://doi.org/10.1109/ISSCC.2018.8310262>
- [22] Chen, Y.-H., Emer, J., Sze, V.: Eyeriss: A spatial architecture for energy-efficient dataflow for convolutional neural networks. In: ACM/IEEE 43rd Annual International Symposium on Computer Architecture (ISCA), pp. 367–379 (2016). <https://doi.org/10.1109/ISCA.2016.40>
- [23] Albericio, J., Delmás, A., Judd, P., Sharify, S., O’Leary, G., Genov, R., Moshovos, A.: Bit-Pragmatic deep neural network computing. In: Proceedings of the 50th Annual IEEE/ACM International Symposium on Microarchitecture. MICRO-50 '17, pp. 382–394. ACM, USA (2017). <https://doi.org/10.1145/3123939.3123982>

- [24] Rokh, B., Azarpeyvand, A., Khanteymooori, A.: A comprehensive survey on model quantization for deep neural networks in image classification. *ACM Transactions on Intelligent Systems and Technology* **14**(6) (2023) <https://doi.org/10.1145/3623402>
- [25] Kulkarni, U., Hosamani, A.S., Masur, A.S., Hegde, S., Vernekar, G.R., Siri Chandana, K.: A survey on quantization methods for optimization of deep neural networks. In: *International Conference on Automation, Computing and Renewable Systems*, pp. 827–834 (2022). <https://doi.org/10.1109/ICACRS55517.2022.10028742>
- [26] Ruta, N., Sawada, N., McKeough, K., Behrisch, M., Beyer, J.: SAX navigator: Time series exploration through hierarchical clustering. In: *2019 IEEE Visualization Conference*, pp. 236–240. IEEE, Canada (2019). <https://doi.org/10.1109/VISUAL.2019.8933618>
- [27] Yu, Y., Becker, T., Trinh, L.M., Behrisch, M.: SAXRegEx: Multivariate time series pattern search with symbolic representation, regular expression, and query expansion. *Computers & Graphics* **112**, 13–21 (2023) <https://doi.org/10.1016/j.cag.2023.03.002>
- [28] Li, X., Lin, J., Zhao, L.: Time series clustering in linear time complexity. *Data Mining and Knowledge Discovery* **35**(6), 2369–2388 (2021) <https://doi.org/10.1007/s10618-021-00798-w>
- [29] Keogh, E., Lin, J., Fu, A.: HOT SAX: efficiently finding the most unusual time series subsequence. In: *IEEE International Conference on Data Mining. ICDM'05*, pp. 1–8 (2005). <https://doi.org/10.1109/ICDM.2005.79>
- [30] Keogh, E., Lonardi, S., Chiu, B.Y.-c.: Finding surprising patterns in a time series database in linear time and space. In: *Proceedings of the 8th ACM SIGKDD International Conference on Knowledge Discovery and Data Mining. KDD '02*, pp. 550–556. ACM, USA (2002). <https://doi.org/10.1145/775047.775128>
- [31] Senin, P., Malinchik, S.: SAX-VSM: Interpretable time series classification using SAX and vector space model. In: *IEEE International Conference on Data Mining*, pp. 1175–1180 (2013). <https://doi.org/10.1109/ICDM.2013.62>
- [32] Li, X., Lin, J.: Linear time complexity time series classification with bag-of-pattern-features. In: *IEEE International Conference on Data Mining*, pp. 277–286 (2017). <https://doi.org/10.1109/ICDM.2017.37>
- [33] Bountrogiannis, K., Tzagkarakis, G., Tsakalides, P.: Distribution agnostic symbolic representations for time series dimensionality reduction and online anomaly detection. *IEEE Transactions on Knowledge and Data Engineering* **35**(6), 5752–5766 (2023) <https://doi.org/10.1109/TKDE.2022.3141158>



- [34] Chen, X.: Joint symbolic aggregate approximation of time series (2024) [2401.00109](#)
- [35] Gray, R.: Vector quantization. *IEEE ASSP Magazine* **1**(2), 4–29 (1984) <https://doi.org/10.1109/MASSP.1984.1162229>
- [36] Dasgupta, S., Freund, Y.: Random projection trees for vector quantization. *IEEE Transactions on Information Theory* **55**(7), 3229–3242 (2009) <https://doi.org/10.1109/TIT.2009.2021325>
- [37] Lloyd, S.: Least squares quantization in PCM. *IEEE Transactions on Information Theory* **28**(2), 129–137 (1982) <https://doi.org/10.1109/TIT.1982.1056489>
- [38] Drineas, P., Frieze, A., Kannan, R., Vempala, S., Vinay, V.: Clustering large graphs via the singular value decomposition. *Machine Learning* **56**(1-3), 9–33 (2004) <https://doi.org/10.1023/B:MACH.0000033113.59016.96>
- [39] Mahajan, M., Nimbhorkar, P., Varadarajan, K.: The planar k-means problem is np-hard. *Theoretical Computer Science* **442**, 13–21 (2012) <https://doi.org/10.1016/j.tcs.2011.12.034> . Special Issue on the Workshop on Algorithms and Computation (WALCOM 2009)
- [40] Yu, S.X., Shi, J.: Multiclass spectral clustering. In: *Proceedings of the Ninth IEEE International Conference on Computer Vision*, vol. 2, p. 313. IEEE, ??? (2003). <https://doi.org/10.1109/ICCV.2003.1238361>
- [41] Ester, M., Kriegel, H.-P., Sander, J., Xu, X.: A density-based algorithm for discovering clusters in large spatial databases with noise. In: *Proceedings of the Second International Conference on Knowledge Discovery and Data Mining. KDD’96*, pp. 226–231. AAAI Press, USA (1996)
- [42] Campello, R.J.G.B., Moulavi, D., Sander, J.: Density-based clustering based on hierarchical density estimates. In: *Advances in Knowledge Discovery and Data Mining*, pp. 160–172. Springer, Germany (2013). [https://doi.org/10.1007/978-3-642-37456-2\\_14](https://doi.org/10.1007/978-3-642-37456-2_14)
- [43] Fränti, P., Sieranoja, S.: How much can k-means be improved by using better initialization and repeats? *Pattern Recognition* **93**, 95–112 (2019) <https://doi.org/10.1016/j.patcog.2019.04.014>
- [44] Saha, J., Mukherjee, J.: CNAK: cluster number assisted k-means. *Pattern Recognition* **110**, 107625 (2021) <https://doi.org/10.1016/j.patcog.2020.107625>
- [45] Jacob, B., Kligys, S., Chen, B., Zhu, M., Tang, M., Howard, A., Adam, H., Kalenichenko, D.: Quantization and training of neural networks for efficient integer-arithmetic-only inference. In: *Proceedings of the IEEE Conference on Computer Vision and Pattern Recognition* (2018). <https://doi.org/10.1109/>

- [46] Sakoe, H., Chiba, S.: Dynamic programming algorithm optimization for spoken word recognition. *IEEE Transactions on Acoustics, Speech, and Signal Processing* **26**(1), 43–49 (1978) <https://doi.org/10.1109/TASSP.1978.1163055>
- [47] Dau, H.A., Bagnall, A., Kamgar, K., Yeh, C.-C.M., Zhu, Y., Gharghabi, S., Ratanamahatana, C.A., Keogh, E.: The UCR time series archive. *IEEE/CAA Journal of Automatica Sinica* **6**(6), 1293–1305 (2019) <https://doi.org/10.1109/JAS.2019.1911747>
- [48] Bagnall, A.J., Dau, H.A., Lines, J., Flynn, M., Large, J., Bostrom, A., Southam, P., Keogh, E.: The UEA multivariate time series classification archive. *CoRR* (2018)
- [49] Arthur, D., Vassilvitskii, S.: **k-means++**: the advantages of careful seeding. In: *SODA '07: Proceedings of the 8th Annual ACM-SIAM Symposium on Discrete Algorithms*, pp. 1027–1035. Society for Industrial and Applied Mathematics, ??? (2007)
- [50] Tan, C.W., Bergmeir, C., Petitjean, F., Webb, G.I.: Time series extrinsic regression: Predicting numeric values from time series data. *Data Mining and Knowledge Discovery* **35**(3), 1032–1060 (2021) <https://doi.org/10.1007/s10618-021-00745-9>
- [51] Jiang, A.Q., Sablayrolles, A., Mensch, A., Bamford, C., Chaplot, D.S., Casas, D.d.l., Bressand, F., Lengyel, G., Lample, G., Saulnier, L., et al.: Mistral 7b. *arXiv preprint arXiv:2310.06825* (2023)
- [52] Dettmers, T., Pagnoni, A., Holtzman, A., Zettlemoyer, L.: QLoRA: Efficient fine-tuning of quantized LLMs. *Advances in Neural Information Processing Systems* **36** (2024)
- [53] Kang, C., Prokop, J., Tong, L., Zhou, H., Hu, Y., Novak, D.: InA: Inhibition adaption on pre-trained language models. *Neural Networks*, 106410 (2024) <https://doi.org/10.1016/j.neunet.2024.106410>
- [54] Paszke, A., Gross, S., Massa, F., Lerer, A., Bradbury, J., Chanan, G., Killeen, T., Lin, Z., Gimelshein, N., Antiga, L., et al.: PyTorch: An imperative style, high-performance deep learning library. *Advances in Neural Information Processing Systems* **32** (2019)
- [55] Jin, M., Wang, S., Ma, L., Chu, Z., Zhang, J.Y., Shi, X., Chen, P.-Y., Liang, Y., Li, Y.-F., Pan, S., Wen, Q.: Time-LLM: Time series forecasting by reprogramming large language models. In: *International Conference on Learning Representations*, Austria (2024)

- [56] Dolan, E.D., Moré, J.J.: Benchmarking optimization software with performance profiles. *Mathematical Programming* **91**(2), 201–213 (2002) <https://doi.org/10.1007/s101070100263>
- [57] Welch, T.A.: A technique for high-performance data compression. *Computer* **17**(6), 8–19 (1984) <https://doi.org/10.1109/MC.1984.1659158>